

DYNAMIC OUTPUT FEEDBACK H_∞ ATTITUDE CONTROL FOR HYPERSONIC GLIDING VEHICLES

WEIDONG ZHANG¹, XIANLIN HUANG¹ AND XIAO-ZHI GAO²

¹Centre of Control Theory and Guidance Technology
Harbin Institute of Technology
No. 92, West Dazhi Street, Nangang District, Harbin 150000, P. R. China
hifinemoment@163.com

²Department of Automation and Systems Technology
School of Electrical Engineering
Aalto University
Helsinki 00076, Finland

Received January 2017; revised May 2017

ABSTRACT. *The problem of robust control for hypersonic gliding vehicle (HGV) with H_∞ performance through dynamic output feedback controller is considered in this paper. The hypersonic vehicle system is high order plant with strong nonlinear coupling parametric uncertainty and external disturbance. In order to handle the complex HGV dynamics, an affine nonlinear plant is transformed to a control-oriented form, which is used as a basic model for the subsequent establishment of T-S fuzzy model. Then based on the approximation and HGV maneuvering in 6DOF, an overall nonlinear T-S fuzzy system with uncertain and disturbance is constructed by parallel distributed compensation (PDC). Further, based on the closed loop system, a robust H_∞ dynamic output feedback controller with complete form that guarantees the closed system stable for the prescribed performance index is designed by a set of strict linear matrix inequality (LMI) conditions. Finally, the designed controller is used to stabilize the HGV attitude system in three channels.*

Keywords: Hypersonic gliding vehicle, H_∞ performance, Dynamic output feedback controller, T-S fuzzy model, Parallel distributed compensation (PDC), Linear matrix inequality (LMI)

1. **Introduction.** Hypersonic gliding vehicle (HGV) is a new class of hypersonic glider being developed nowadays which is shown to endure strongly nonlinear dynamic behavior over the flight envelope between 120Km and 30Km. The vehicle is generally launched by boosters from the ground or released from the space orbiter, and glides inside the atmosphere even more than ten thousand kilometers. As the typical HGVs, such as CAV (common aero vehicle) [1], HTV (hypersonic technology vehicle) [2], and IGLA [3], possess the capabilities of rapid response, strong penetration, good maneuverability and global reach, HGVs have been regarded as the advanced precision-guided weapon with important strategic deterrent and tactical strike, and being researched and developed by the world especially military powers, which indicates a significant scientific value and military and political significance.

In the extant studies on HGVs, much attention has been paid to the trajectory optimization and guidance [4-6]; however, the reentry attitude control issue is explored in depth [7-10], which shows important value for further research. Compared with traditional aircraft, HGVs have greater flight envelope, and more diverse aerodynamic heat and aerodynamic force uncertainties brought from more complex atmospheric environment, additionally, greater flight speed and shape layout make the structure of the aerodynamic parameters

more diversified and complicated. On the other hand, HGVs are extremely sensitive to changes of atmospheric conditions as well as dynamics and aerodynamic parameters during the reentry period. These characteristics pose a significant challenge for the system control, such as bringing problems of strong nonlinearity and fast time-varying parameters, strong coupling for model states and parameters, and uncertainty and disturbance of the model.

To deal with these problems, various nonlinear control methodologies have subsequently been developed and applied to the study of hypersonic vehicles [7-15], such as backstepping control, linear parameter-varying control and adaptive sliding mode control schemes. In [8], the LPV-LFT method is applied to designing an angle-of-attack tracking control system whose aerodynamic parameters vary dramatically during reentry phase. In [11], Xu provides adaptive dynamic surface control for the flexible model of hypersonic flight vehicle in the presence of unknown dynamics and input nonlinearity. Direct neural control with robust design is used to avoid singularity, and the uniform ultimate boundedness stability of the closed-loop system is guaranteed. In [15], a multi-input/multi-output adaptive sliding controller is designed and analyzed to solve the problems of nonlinear, multivariable, and unstable and includes uncertain parameters for a longitudinal dynamics of a generic hypersonic air vehicle.

However, these nonlinear control schemes require the nonlinear systems present predictable behaviors, such as minimum-phase characteristics and precisely available parameters, which limit practical applications for HGVs. For the high nonlinear dynamics of hypersonic vehicles, the control scheme is still an open and challenging problem, including when uncertainties and disturbances exist simultaneously.

Since the T-S fuzzy control theory was put forward in 1989, a large amount of developments have been achieved during recent decades. In fact, the T-S fuzzy models have shown to be universal function approximators in the sense that they can approximate any smooth nonlinear function to any degree of accuracy in any convex, compact region [16-18]. Until now, the T-S fuzzy control theory, including the fuzzy modeling technology based on universal approximation and the feedback control technology based on Lyapunov stability theory, has been well studied and employed both in traditional engineering systems [19-22] and the hypersonic vehicle control systems [23-27]. In [25], a fuzzy guaranteed cost state feedback controller is designed to stabilize the obtained T-S fuzzy system based on the longitudinal model of a flexible air-breathing hypersonic vehicle (FAHV). In [26], a fuzzy multi-objective robust controller is developed by deriving a linear matrix inequality (LMI) sufficient condition for fuzzy singularly perturbed models (FSPM) for the longitudinal motion of an air-breathing hypersonic vehicle.

Although these works can effectively solve some hypersonic vehicle problems or even be applied in HGV control system, most of the above mentioned results are with the assumption that the full system states are measurable. In fact, during the flight period, the system states are not entirely measurable as the harsh atmospheric environment and vehicle constraints. Therefore, conditions for designing controllers via measurable output information are explored. Thus, the output feedback control strategy presents highly significance for HGV control.

Generally, three output feedback control approaches are available for system output stabilization design: state observer, static output feedback and dynamic output feedback. The state observer approach is interesting when the state is not entirely available and premises variables are measurable so that a separation principle can be available. The static output feedback approach is considered to reduce real-time computational cost because of its concise form and can be easily realized in practice; however, the controller parameters conditions are difficult to be transformed in terms of LMI but the BMI [28].

The dynamic output feedback approach can provide more parameters and flexible choice for controller design. As the static output feedback control for linear time-invariant (LTI) systems is still an open problem, and the dynamic output feedback problem of LTI systems has been solved by an LMI-based sufficient and necessary condition [29], although dynamic output feedback problems can be transformed into static output feedback problems, it is more necessary to study dynamic output feedback problems but static output feedback problems for T-S fuzzy systems.

Among the available literature, the dynamic output feedback controller has been designed for the continuous and discrete-time switched systems to render the associated closed-loop switched linear system globally asymptotically stable [30,31]. For the studies of hypersonic vehicle system design with dynamic output feedback control in longitudinal model, numerous approaches are exploited to address for the velocity and altitude tracking [32-36]. Li et al. [32] design an output feedback controller that yields semiglobal uniformly ultimately bounded tracking of the velocity and altitude while keeping all the closed loop signals bounded for a generic hypersonic vehicle, where high gain observers (HGO) are utilized to estimate derivatives of the velocity and altitude, and neural network based feed forward function is designed to compensate for model uncertainties. In [33], Zong et al. adopted a combined nonlinear observer and back-stepping technique to design the dynamic output feedback controller that provides stable tracking of the velocity and altitude reference trajectories by small-gain theorem for the nonlinear longitudinal dynamics of a generic hypersonic vehicle. In [34], the authors provide robust output-feedback controller for a model of an airbreathing hypersonic vehicle by an alternative approach to robust output-feedback design that does not employ state estimation to track velocity and altitude signal in the presence of model uncertainties and varying flight condition.

Although the longitudinal model control of hypersonic vehicle has been deeply researched, the control schemes of the dynamic model in three channels or the motion plant in full 6DOF, such as the HGVs and GHVs (generic hypersonic vehicles), are still far from fully explored, especially based on dynamic output feedback strategy, there is hardly any investigation so far.

Multiple control strategies have been investigated for the HGV system, such as back-stepping control [7], LPV control [8] and adaptive control [11,37], and characteristic model approach [9] is used to handle the complex plant. In [7], the authors employed a robust dynamic inversion control approach to deal with the parameter perturbations, high uncertainties and strong couplings during the flight of hypersonic gliding vehicle. In [9], Luo and Li introduce the fuzzy logic into the characteristic modeling by dividing the whole restriction range into several subspaces, and a new intelligent controller is proposed to solve the problem of longitudinal attitude control of hypersonic vehicle in gliding phase. On the other hand, for the uncertainty and disturbance, observer method is designed for the system. The observer approaches in [10,38,39] are used to estimate the uncertainty or disturbance and the state feedback control is employed for HGVs. In [10], Qian et al. used a nonlinear disturbance observer (NDO) to estimate the unknown disturbance which is then integrated with a conventional sliding mode controller for HGV control. In [38], Gao proposed an observer-based approach to obtain the exact values of the parameters in the kinetic model, and nonlinear dynamic inversion controller is designed for the longitudinal dynamic model of HGV.

Although these methods solve the HGV control problem to a certain extent, it is difficult to be applied directly in practice by state feedback, and the observer-based method also brings difficulty for the complex system synthesis. Therefore, under these circumstances, it is much necessary to pay more attention to the output feedback control design for HGV

system with parameter uncertainty and external disturbances, especially by fuzzy control strategy. This makes up the motivation of this paper.

Summarizing, the main contributions in this paper are to provide the T-S fuzzy model of HGV three-channel attitude dynamics, and firstly introduce dynamic output feedback controller with complete form by T-S fuzzy control strategy to address the problem of HGV attitude control in three channels, and a new sufficient condition to ensure system performance through strict LMIs is proposed. This paper is organized as follows. In Section 2, the system description is presented and the problem of dynamic controller design is raised. In Section 3, we construct the closed loop control system with the presented T-S fuzzy model and dynamic output controller. In Section 4, the robust H_∞ dynamic output feedback controller is provided to stabilize the presented uncertain closed loop control system for a prescribed performance. Simulation results are given in Section 5. Finally, concluding remarks are made in Section 6.

2. Problem Formulation. Hypersonic vehicle is a complex nonlinear system with multi-state, strong coupling and strong time-varying. The reentry dynamics present as the form of differential equation with multiple variables and structures, which is not conducive to the analysis of the control system because of the lack of necessary control structure. In order to solve this problem, in this section the dynamics model is transformed into a control-oriented affine nonlinear form.

2.1. Reentry dynamics. The original nonlinear reentry attitude equations of the hypersonic vehicle can be described as follows [40]:

$$\begin{cases} \dot{\alpha} = q - \tan \beta(p \cos \alpha + r \sin \alpha) - \frac{\cos \mu}{\cos \beta} \frac{F_\gamma}{MV} + \frac{\cos \mu}{\cos \beta} \frac{F_\chi}{MV} \\ \dot{\beta} = p \sin \alpha - r \cos \alpha + \sin \mu \frac{F_\gamma}{MV} + \cos \mu \frac{F_\chi}{MV} \\ \dot{\mu} = -q \sin \beta - \cos \beta(p \cos \alpha + r \sin \alpha) + \dot{\alpha} \sin \beta - \frac{F_\chi}{MV} \tan \gamma \\ \dot{p} = I_{pq}^p pq + I_{qr}^p qr + g_n^p n + g_l^p l \\ \dot{q} = I_{pp}^q p^2 + I_{rr}^q r^2 + I_{pr}^q pr + g_m^q m \\ \dot{r} = I_{qr}^r qr + I_{pq}^r pq + g_l^r l + g_n^r n \end{cases} \quad (1)$$

Here, α, β, μ denote the angle of attack, sideslip angle, and bank angle, respectively; p, q, r denote the bank angle rate of rotation, angle of attack rate, and sideslip angle rate of rotation, respectively. F_γ, F_χ denote force functions associated with aerodynamic drag, lift and side forces.

So the affine nonlinear model of (1) can be obtained as:

$$\dot{\Omega} = f_s + g_{s1}\omega + g_{s2}\delta \quad (2)$$

$$\dot{\omega} = f_f + g_f M_c = f_f + g_f \cdot g_{f\delta} \delta \quad (3)$$

where

$$f_s = \frac{1}{MV} \begin{bmatrix} \frac{-C_{L,\alpha}QS + Mg \cos \gamma \cos \mu}{\cos \beta} \\ -C_{Y,\beta}\beta QS - Mg \cos \gamma \sin \mu \\ C_{L,\alpha}QS(\tan \beta + \cos \mu) + C_{Y,\beta}\beta QS \cos \beta \\ -Mg \cos \gamma \cos \mu \tan \beta \end{bmatrix},$$

$$g_{s1} = \begin{bmatrix} -\tan \beta \cos \alpha & 1 & -\tan \beta \sin \alpha \\ \sin \alpha & 0 & -\cos \alpha \\ -\sec \beta \cos \alpha & 0 & -\sec \beta \sin \alpha \end{bmatrix},$$

$$\mathbf{f}_f = \begin{bmatrix} I_{pq}^p pq + I_{qr}^p qr + g_l^p l_A \\ I_{pp}^q p^2 + I_{rr}^q r^2 + I_{pr}^q pr + g_m^q m_A \\ I_{qr}^r qr + I_{pq}^r pq + g_l^r n_A \end{bmatrix}, \mathbf{g}_f = \begin{bmatrix} g_l^p & 0 & g_n^p \\ 0 & g_m^q & 0 \\ g_l^r & 0 & g_n^r \end{bmatrix}, \boldsymbol{\delta} = \begin{bmatrix} \delta_e \\ \delta_a \\ \delta_r \end{bmatrix}$$

In particular, as the aerodynamic force generated by the rudder deflection is far less than the force generated by the vehicle body, $\mathbf{g}_{s2}\boldsymbol{\delta}$ has a negligible effect on variables $\boldsymbol{\Omega} = [\alpha, \beta, \mu]^T$. Therefore, recasting Equation (2) yields

$$\dot{\boldsymbol{\Omega}} = \mathbf{f}_s + \mathbf{g}_{s1}\boldsymbol{\omega} \tag{4}$$

From Equations (3) and (4), it yields

$$\begin{bmatrix} \dot{\boldsymbol{\Omega}} \\ \dot{\boldsymbol{\omega}} \end{bmatrix} = \begin{bmatrix} \mathbf{g}_{s1}\boldsymbol{\omega} \\ \mathbf{f}_{f1} \end{bmatrix} + \begin{bmatrix} \mathbf{0} \\ \mathbf{g}_f \end{bmatrix} \mathbf{M}_c + \begin{bmatrix} \mathbf{f}_s \\ \mathbf{f}_{f2} \end{bmatrix}$$

Let $\mathbf{x}(t) = [\boldsymbol{\Omega}^T, \boldsymbol{\omega}^T]^T = [\alpha, \beta, \mu, p, q, r]^T$, $\begin{bmatrix} \mathbf{g}_{s1}\boldsymbol{\omega} \\ \mathbf{f}_{f1} \end{bmatrix}_{6 \times 1} = \mathbf{f}(x)$, $\begin{bmatrix} \mathbf{0}_{3 \times 3} \\ \mathbf{g}_f \end{bmatrix}_{6 \times 3} = \mathbf{g}(x)$,

$(\mathbf{M}_c)_{3 \times 1} = \mathbf{u}(t)$, $\begin{bmatrix} \mathbf{f}_s \\ \mathbf{f}_{f2} \end{bmatrix}_{6 \times 1} = \boldsymbol{\Delta}(x)$.

Finally, the nonlinear affine model can be rewritten as

$$\dot{\mathbf{x}}(t) = \mathbf{f}(x) + \mathbf{g}(x)\mathbf{u}(t) + \boldsymbol{\Delta}(x) \tag{5}$$

in which

$$\mathbf{f}(x) = \begin{bmatrix} -p \tan \beta \cos \alpha + q - r \tan \beta \sin \alpha \\ p \sin \alpha - r \cos \alpha \\ -p \sec \beta \cos \alpha - r \sec \beta \sin \alpha \\ I_{pq}^p pq + I_{qr}^p qr \\ I_{pp}^q p^2 + I_{rr}^q r^2 + I_{pr}^q pr \\ I_{qr}^r qr + I_{pq}^r pq \end{bmatrix} \triangleq \begin{bmatrix} f_1 \\ f_2 \\ f_3 \\ f_4 \\ f_5 \\ f_6 \end{bmatrix}, \mathbf{g}(x) = G = \begin{bmatrix} \mathbf{0}_{3 \times 3} \\ g_l^p & 0 & g_n^p \\ 0 & g_m^q & 0 \\ g_l^r & 0 & g_n^r \end{bmatrix}$$

$$\boldsymbol{\Delta}(x) = \begin{bmatrix} \frac{-C_{L\alpha}QS + Mg \cos \gamma \cos \mu}{MV \cos \beta} \\ \frac{-C_{Y\beta}\beta QS - Mg \cos \gamma \sin \mu}{MV} \\ \frac{C_{L\alpha}QS(\tan \beta + \cos \mu) + C_{Y\beta}\beta QS \cos \beta - Mg \cos \gamma \cos \mu \tan \beta}{MV} \\ g_l^p l_A + g_n^p n_A \\ g_m^q m_A \\ g_l^r l_A + g_n^r n_A \end{bmatrix}$$

Here, $\boldsymbol{\Delta}(x)$ is considered as an uncertainty term related to the vehicle's aerodynamic parameters. $\mathbf{u}(t)$ is a control variable with respect to the control surface deflections.

Figure 1 provides the zero input response for the original plant (5) at initial states $\mathbf{x}(0) = [0, 0, 0, 0.1, 0, 0]^T$ and $\mathbf{x}(0) = [0, 0, 0, 0, 0, 0.1]^T$, it can be seen that the attitude angle of the system exhibits a fast divergent state for the open loop system, while the attitude angular rate exhibits a characteristic of oscillating divergence. It can be seen that the original system dynamics has strong coupling and nonlinearity, which is not conducive to the direct controller design.

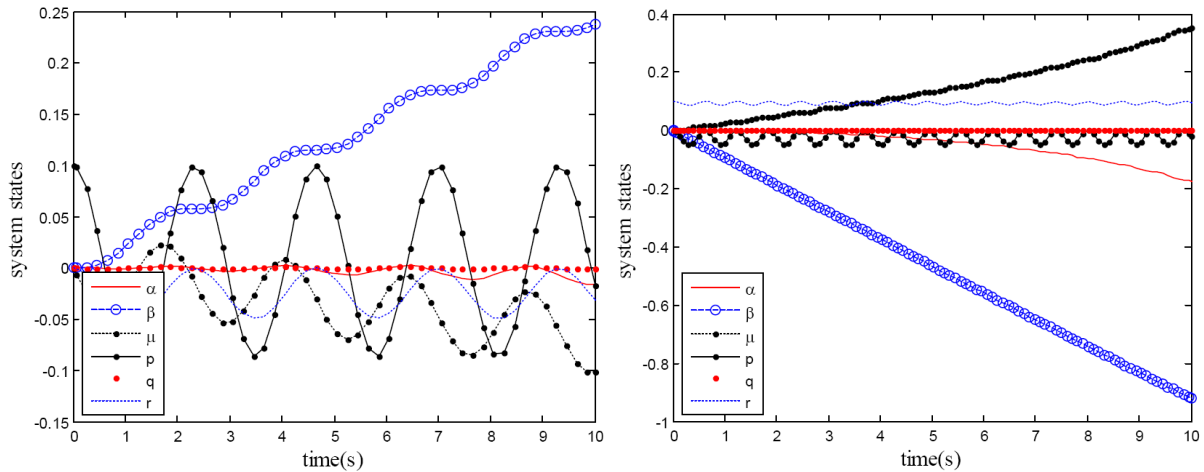


FIGURE 1. Zero input response for the original plant in different initial states

2.2. T-S fuzzy modeling. Since our aim is to complete the controller design of the attitude dynamics, although the control-oriented affine nonlinear model has been given and the original dynamic model structure has been simplified, it can be seen that the affine model still has strong nonlinear and time-varying characteristics, and it is still difficult to design the control system directly. However, if we adopt the T-S fuzzy modeling technology to construct an intermediate fuzzy model for the original plant, the difficulty of designing the closed-loop controller will be greatly reduced. Therefore, it is necessary to establish the T-S fuzzy model of the original system.

In this section, the reentry dynamics model shown in (9) is transformed into a fuzzy combination of local linear submodels by T-S fuzzy modeling techniques. The blending nonlinear fuzzy model is constructed by the selected operating points of interest shown in Table 1.

TABLE 1. The selected operating points of interest

Points	Values
\mathbf{x}^1	$[0, 0, 0, -p_m, 0, -r_m]^T$
\mathbf{x}^2	$[0, 0, 0, -p_m, 0, 0]^T$
\mathbf{x}^3	$[0, 0, 0, -p_m, 0, r_m]^T$
\mathbf{x}^4	$[0, 0, 0, 0, 0, -r_m]^T$
\mathbf{x}^5	$[0, 0, 0, 0, 0, 0]^T$
\mathbf{x}^6	$[0, 0, 0, 0, 0, r_m]^T$
\mathbf{x}^7	$[0, 0, 0, p_m, 0, -r_m]^T$
\mathbf{x}^8	$[0, 0, 0, p_m, 0, 0]^T$
\mathbf{x}^9	$[0, 0, 0, p_m, 0, r_m]^T$

Note that considering the fuzzy model, this paper constructs an aircraft model in three channels, so as the open response tests provide in Figure 1, we found the variables of bank angle rate and sideslip angle rate have a decisive effect on the severe nonlinearity and response divergence of the original dynamics. Therefore, in order to accurately describe

these nonlinear dynamics by fuzzy model, the variables of bank rate and sideslip rate are chosen for the premise variables.

In addition, in order to accurately express the maneuvering behaviors of the vehicle in these two channels, three state points are chosen in each channel, which respectively represents, for instance the bank angle channel, the three maneuvers of left, right and unmaneuver. The other channel cases are similar. Therefore, from the analysis above, a total of nine operating points of interest are selected, which correspond to nine fuzzy rules described as follows.

Rule i : If p is about p_k^i rad/s and r is about r_l^i rad/s, $k, l = 1, 2, 3$
Then,

$$\begin{cases} \dot{\mathbf{x}} = (A_i + \Delta A_i)\mathbf{x} + (B_i + \Delta B_{1i})\mathbf{u} + B_{2i}\omega & i = 1, 2, \dots, 9 \\ \mathbf{z} = E_i\mathbf{x} \\ \mathbf{y} = C_i\mathbf{x} \end{cases} \quad (6)$$

where $p_k^i \in \{-p_m, 0, p_m\}$, $r_l^i \in \{-r_m, 0, r_m\}$, p_m and r_m are the maximum value of the rotation angular rate p and r , and the state point formed by each rule in turn corresponds to the operating point in Table 1. z is the controlled output. y is the measured output. ω is the disturbance input. The uncertainties considered in this paper are norm-bounded and described by $[\Delta A_i \ \Delta B_{1i}] = M_i F_i [N_{1i} \ N_{2i}]$, where ΔA_i , M_i , N_{1i} , N_{2i} are known real constant matrices of appropriate dimensions and F_i is nonlinear time-varying matrix functions satisfying $F_i^T F_i \leq I$.

Based on the Jacobi linearization and fuzzy linearization method [41], the calculation of local matrix for submodels can be divided in two cases as follows.

For the zero equilibrium point \mathbf{x}^5 , according to the Jacobi linearization method,

$$A_j = J(\mathbf{f}(\mathbf{x}^j)), \quad B_{1i} = G \quad (7)$$

For the other operating points except \mathbf{x}^5 shown in Table 1, the fuzzy linearization method will be applied as

$$A_j = J(\mathbf{f}(\mathbf{x}^j)) + [\mathbf{x}^j \cdot Z_j]^T \quad (8)$$

$$B_{1i} = G$$

where $Z_j \triangleq \frac{1}{\|\mathbf{x}^j\|^2} \left([\mathbf{f}(\mathbf{x}^j)]^T - (\mathbf{x}^j)^T [J(\mathbf{f}(\mathbf{x}^j))]^T \right)$, $J(\mathbf{f}) = \frac{\partial \mathbf{f}}{\partial \mathbf{x}}$.

The subsystem matrices and control matrices (see Appendix) were separately modeled at the operating points of interest shown in Table 1.

By the PDC, the blending nonlinear T-S fuzzy model with uncertain and disturbance can be constructed as

$$\begin{cases} \dot{\mathbf{x}} = \sum_{i=1}^9 \mu_i [(A_i + \Delta A_i)\mathbf{x} + (B_{1i} + \Delta B_{1i})\mathbf{u} + B_{2i}\omega] \\ \mathbf{z} = E\mathbf{x} \\ \mathbf{y} = C\mathbf{x} \end{cases} \quad (9)$$

where $\mu_i(t) = \frac{m_i(t)}{\sum_{i=1}^r m_i(t)}$, $m_i(\mathbf{z}(t)) = \prod_{j=1}^l M_{ij}(\mathbf{z}_j(t))$.

The model (9) will be used as an intermediate model of the original system (5). In the next section, for the controller design, we will composite the T-S model into a closed loop system with dynamic output feedback controller.

3. Dynamic Output Feedback Control. Figure 2 shows the basic principles of dynamic output feedback control. In the general dynamic output feedback studies [30, 42], the output controller parameter matrix only contains A_c , B_c , C_c without the observation matrix D_c . This paper firstly introduces T-S fuzzy dynamic output feedback controller with observation matrix into the design of HGV attitude control in three channels. Thereby the degree of freedom of the parameter design is increased so that controller design of the conservatism is reduced.

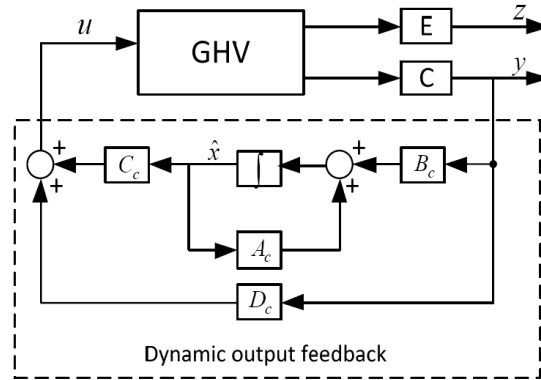


FIGURE 2. Basic structure of dynamic output feedback control

The full-order fuzzy dynamic output feedback controller with a complete form for the fuzzy system (6) is constructed as

Rule i : If p is about p_k^i rad/s and r is about r_l^i rad/s, $k, l = 1, 2, 3$

Then

$$\begin{cases} \dot{\hat{x}} = A_{ci}\hat{x} + B_{ci}y \\ u = C_{ci}\hat{x} + D_{ci}y \end{cases} \quad (10)$$

where $\hat{x} \in \mathbf{R}^n$ is the controller state. y is the measurable output, and u is the control output. $A_{ci}, B_{ci}, C_{ci}, D_{ci}$ are the controller parameter matrices to be determined.

From (9) and (10), the closed loop system with controller states can be described as:

$$\begin{cases} \begin{bmatrix} \dot{x} \\ \dot{\hat{x}} \end{bmatrix} = \sum_{i=1}^9 \sum_{j=1}^9 \mu_i \mu_j \left\{ \begin{bmatrix} A_i + B_{1i}D_{cj}C & B_{1i}C_{cj} \\ B_{cj}C & A_{cj} \end{bmatrix} \right. \\ \quad \left. + \begin{bmatrix} \Delta A_i + \Delta B_{1i}D_{cj}C & \Delta B_{1i}C_{cj} \\ 0 & 0 \end{bmatrix} \begin{bmatrix} x \\ \hat{x} \end{bmatrix} + \begin{bmatrix} B_{2i} \\ 0 \end{bmatrix} \omega \right\} \\ z = [E \quad 0] \begin{bmatrix} x \\ \hat{x} \end{bmatrix} \end{cases} \quad (11)$$

or equivalently, shown as

$$\begin{cases} \dot{\aleph}(t) = (A_{e\mu} + \Delta A_{e\mu}) \aleph(t) + B_{2\mu}\omega(t) \\ z(t) = E_e \aleph(t) \end{cases} \quad (12)$$

where $\aleph = \begin{bmatrix} x \\ \hat{x} \end{bmatrix}$ is the closed-loop system state, $A_{e\mu} = \sum_{i=1}^9 \sum_{j=1}^9 \mu_i \mu_j A_{eij}$ is the closed-loop system matrix, $\Delta A_{e\mu} = \sum_{i=1}^9 \sum_{j=1}^9 \mu_i \mu_j \Delta A_{eij}$ is the closed-loop system uncertainty matrix,

$B_{2\mu} = \sum_{i=1}^9 \mu_i B_{2eij}$ is the disturbance matrix, $E_e = [E \quad 0]$ is the closed-loop system

controlled output matrix, and

$$A_{eij} = \begin{bmatrix} A_i + B_{1i}D_{cj}C & B_{1i}C_{cj} \\ B_{cj}C & A_{cj} \end{bmatrix},$$

$$\Delta A_{eij} = \begin{bmatrix} \Delta A_i + \Delta B_{1i}D_{cj}C & \Delta B_{1i}C_{cj} \\ 0 & 0 \end{bmatrix} = M_{eij}F_{eij}N_{eij}, \quad B_{2eij} = \begin{bmatrix} B_{2i} \\ 0 \end{bmatrix},$$

$$M_{eij} = \begin{bmatrix} M_i & 0 \\ 0 & 0 \end{bmatrix}, \quad F_{eij} = \begin{bmatrix} F_i & 0 \\ 0 & 0 \end{bmatrix}, \quad N_{eij} = \begin{bmatrix} N_{1i} + N_{2i}D_{cj}C & N_{2i}C_{cj} \\ 0 & 0 \end{bmatrix}.$$

For the uncertain T-S fuzzy model represented in (12), the robust H_∞ performance can be defined as follows.

Definition 3.1. *Given a real number $\gamma > 0$, the uncertain T-S fuzzy system (12) is said to be robustly stable with γ disturbance attenuation if, for all allowable uncertainties and for any $\omega(t) \in L_2(0, \infty)$, system (12) is stable and the response $z(t)$, under zero initial condition, satisfies the following equation*

$$\int_0^{+\infty} z(t)^T z(t) d\tau < \gamma^2 \int_0^{+\infty} \omega(t)^T \omega(t) d\tau \tag{13}$$

or the equivalent form

$$\frac{\|z(t)\|_2}{\|\omega(t)\|_2} < \gamma$$

Then, our objective is to achieve the controller gains $(A_{ci}, B_{ci}, C_{ci}, D_{ci})$ in (10) such that the closed-loop system in (12) is asymptotically stable with γ -disturbance attenuation.

4. Robust H_∞ Controller Design. In this section, a set of LMI conditions is derived for designing the dynamic output feedback controller (10). For finding the controllers, the following lemmas are needed.

Lemma 4.1. [43] *Let X, Y , and F be real matrices with appropriate dimensions and $FF^T \leq I$. Then for any scalar $\varepsilon > 0$,*

$$XFY + Y^T F^T X^T \leq \varepsilon XX^T + \frac{1}{\varepsilon} YY^T \tag{14}$$

Lemma 4.2. [44] *The parameterized linear matrix inequality*

$$\sum_{i,j=1}^r \mu_i \mu_j \bar{M}_{ij} < 0 \tag{15}$$

is fulfilled, if the following condition holds:

$$\begin{cases} \bar{M}_{ii} < 0 & i = 1, \dots, r \\ \frac{1}{r-1} \bar{M}_{ii} + \frac{1}{2} (\bar{M}_{ij} + \bar{M}_{ji}) < 0 & 1 \leq i \neq j \leq r \end{cases} \tag{16}$$

Theorem 4.1. [36] *For the uncertain T-S fuzzy system (12), if there exist a matrix $P > 0$ and a scalar $\varepsilon > 0$ satisfying*

$$\sum_{i=1}^9 \sum_{j=1}^9 \mu_i \mu_j \begin{bmatrix} PA_{eij} + A_{eij}^T P + E_e^T E_e + \varepsilon N_{eij}^T N_{eij} & PD_e & PM_i \\ * & -\gamma^2 I & 0 \\ * & * & -\varepsilon I \end{bmatrix} < 0 \tag{17}$$

then the system in Equation (12) is robustly stable and the H_∞ performance in Equation (13) is guaranteed for a prescribed performance index γ .

Applying the Schur complement to Equation (17) (the right part of $\sum_{i=1}^9 \sum_{j=1}^9 \mu_i \mu_j$) in Theorem 4.1, the following equivalent inequalities can be obtained

$$\begin{aligned} & (PA_{eij} + A_{eij}^T P + E_e^T E + \varepsilon N_{eij}^T N_{eij}) \\ & - \begin{bmatrix} PB_{2eij} & PM_{eij} \end{bmatrix} \begin{bmatrix} -\gamma^{-2}I & 0 \\ * & -\varepsilon^{-1}I \end{bmatrix} \begin{bmatrix} (PB_{2eij})^T \\ (PM_{eij})^T \end{bmatrix} < 0 \end{aligned} \tag{27}$$

It is easy to derive Formula (27) into the equivalent form

$$\begin{aligned} & PA_{eij} + A_{eij}^T P - PB_{2eij} (-\gamma^2 I)^{-1} B_{2eij}^T P - PM_{eij} (-\varepsilon I)^{-1} M_{eij}^T P \\ & - N_{eij}^T (-\varepsilon^{-1} I)^{-1} N_{eij} - E_e^T (-I) E_e < 0 \end{aligned} \tag{28}$$

Applying the Schur complement again to Formula (28), it is equivalent to

$$\begin{aligned} & PA_{eij} + A_{eij}^T P - \begin{bmatrix} PB_{2eij} & PM_{eij} & N_{eij}^T & E_e^T \end{bmatrix} \begin{bmatrix} -\gamma^2 I & & & \\ & -\varepsilon I & & \\ & & -\varepsilon^{-1} I & \\ & & & -I \end{bmatrix}^{-1} \\ & \begin{bmatrix} PB_{2eij} & PM_{eij} & N_{eij}^T & E_e^T \end{bmatrix}^T < 0 \end{aligned} \tag{29}$$

Applying the Schur complement for the third time to Formula (29), it can be derived as

$$\begin{bmatrix} PA_{eij} + A_{eij}^T P & PB_{2eij} & PM_{eij} & N_{eij}^T & E_e^T \\ * & -\gamma^2 I & 0 & 0 & 0 \\ * & * & -\varepsilon I & 0 & 0 \\ * & * & * & -\varepsilon^{-1} I & 0 \\ * & * & * & * & -I \end{bmatrix} < 0 \tag{30}$$

Therefore, the overall form can be expressed as follows

$$\sum_{i=1}^9 \sum_{j=1}^9 \mu_i \mu_j \begin{bmatrix} PA_{eij} + A_{eij}^T P & PB_{2eij} & PM_{eij} & N_{eij}^T & E_e^T \\ * & -\gamma^2 I & 0 & 0 & 0 \\ * & * & -\varepsilon I & 0 & 0 \\ * & * & * & -\varepsilon^{-1} I & 0 \\ * & * & * & * & -I \end{bmatrix} < 0 \tag{31}$$

Pre- and post-multiplying Equation (31) by $diag(T_1^T, I, I, I, I, I)$ and $diag(T_1, I, I, I, I, I)$, we obtain

$$\sum_{i=1}^9 \sum_{j=1}^9 \mu_i \mu_j \begin{bmatrix} T_1^T (PA_{eij} + A_{eij}^T P) T_1 & T_1^T PB_{2eij} & T_1^T PM_{eij} & T_1^T N_{eij}^T & T_1^T E_e^T \\ * & -\gamma^2 I & 0 & 0 & 0 \\ * & * & -\varepsilon I & 0 & 0 \\ * & * & * & -\varepsilon^{-1} I & 0 \\ * & * & * & * & -I \end{bmatrix} < 0 \tag{32}$$

Equation (32) can be derived as

$$\sum_{i,j=1}^r \mu_i \mu_j \Theta_{ij} < 0 \tag{33}$$

where Θ_{ij} is shown as Equation (21) and X_j, Y_j, Z_j, W_j are expressed as

$$D_{cj} C G_1 + C_{cj} G_2^T = X_j \tag{34}$$

$$P_1 B_{1i} D_{cj} + P_2 B_{cj} = Y_j \tag{35}$$

$$P_1 A_i G_1 + P_1 B_{1i} D_{cj} C G_1 + P_2 B_{cj} C G_1 + P_1 B_{1i} C_{cj} G_2^T + P_2 A_{cj} G_2^T = Z_j \tag{36}$$

$$D_{cj} = W_j \tag{37}$$

Inversing these Equations (31)-(34), Equations (22)-(25) can be obtained. Finally, by Lemma 4.2, Equations (19) and (20) can be easily obtained.

The proof is completed.

Remark 4.1. Equation (21) provides a complete explicit form of the matrix in Formula (32) after derivation. Equations (34)-(37) provide the new defined matrix variables that aim to transform the matrix in Formula (32) into a linear matrix form in the derivation process so that the final sufficient conditions can be shown as strict LMI forms. Specifically, for example, the matrix block $T_1^T (P A_{eij} + A_{eij}^T P) T_1$ in Formula (32) can be derived as

$$\begin{aligned} & T_1^T (P A_{eij} + A_{eij}^T P) T_1 \\ = & \begin{bmatrix} A_i G_1 + B_{1i} (D_{cj} C G_1 + C_{cj} G_2^T) & A_i + B_{1i} D_{cj} C \\ P_1 A_i G_1 + P_1 B_{1i} D_{cj} C G_1 + P_2 B_{cj} C G_1 & P_1 A_i + (P_1 B_{1i} D_{cj} + P_2 B_{cj}) C \\ + P_1 B_{1i} C_{cj} G_2^T + P_2 A_{cj} G_2^T & \end{bmatrix} + * \end{aligned}$$

As long as the matrix variables are set as (34)-(37), the matrix blocks shown in Equation (21) can be obtained as

$$\begin{bmatrix} A_i G_1 + B_{1i} X_j + (A_i G_1 + B_{1i} X_j)^T & A_i + B_{1i} W_j C + Z_i^T \\ Z_i + (A_i + B_{1i} W_j C)^T & P_1 A_i + Y_j C + (P_1 A_i + Y_j C)^T \end{bmatrix}$$

Similarly, the blocks $T_1^T P B_{2eij}$, $T_1^T P M_{eij}$, $T_1^T N_{eij}^T$, $T_1^T E_e^T$ in Formula (32) follow the same principle as above.

5. Simulation Results. In this part, stabilization of attitude control is tested with the output feedback controller by using Theorem 4.2. Respectively, select the operating points and the points within domains to detect the output stability of the attitude.

Taking account of the maneuverability of the HGV, set the parameter in Formula (6) as $p_m = r_m = \pi/18$ rad/s, which is reasonable maneuverability value for HGV [45]. Assume that the attitude angle $[\alpha, \beta, \mu]$ is measurable, and make the measurable variables as the controlled output, so that the output matrices and controlled output matrices are set as follows:

$$C = \begin{bmatrix} 1 & 0 & 0 & 0 & 0 & 0 \\ 0 & 1 & 0 & 0 & 0 & 0 \\ 0 & 0 & 1 & 0 & 0 & 0 \end{bmatrix}, \quad E = \begin{bmatrix} 1 & 0 & 0 & 0 & 0 & 0 \\ 0 & 1 & 0 & 0 & 0 & 0 \\ 0 & 0 & 1 & 0 & 0 & 0 \end{bmatrix}.$$

Since in Equation (5), each dimension of $f(x)$ may show parameter uncertainty, we set some uncertainty for each dimension. Assume the control input parameter uncertainty exists only in the attitude angle channel (first three dimensions), so that the uncertainty matrices can be set as follows:

$$M = \text{diag}(0.01, 0.01, 0.01, 0.01, 0.01, 0.01), \quad N_1 = \text{diag}(0.01, 0.01, 0.01, 0.01, 0.01, 0.01)$$

$$N_2 = \begin{bmatrix} 0.01 & 0 & 0 \\ 0 & 0.01 & 0 \\ 0 & 0 & 0.01 \\ 0 & 0 & 0 \\ 0 & 0 & 0 \\ 0 & 0 & 0 \end{bmatrix}$$

Assume the disturbance exists in each state dimension, set disturbance matrix as: $D = [1 \ 1 \ 1 \ 1 \ 1 \ 1]^T$, $\omega(t) = \begin{cases} 0.1 & 5 \leq t \leq 6 \\ 0 & \text{others} \end{cases}$. This result shows the response at a basic operating point $x^2 = [0 \ 0 \ 0 \ -\pi/18 \ 0 \ 0]$ and at an extended maneuvering state $[0.05 \ 0 \ 0.01 \ -\pi/18 \ 0 \ 0]$. In order to better illustrate the performance of this designed controller, it is compared with the controller in [36] in which only the basic construction without the matrix D_{c_j} is designed. For better clarification, the two controllers are described as follows:

Controller I: the designed controller in [36];

Controller II: the designed controller in Theorem 4.2.

Figures 3-6 show the response of system attitude angle and attitude angular rate at points $x^2 = [0 \ 0 \ 0 \ -\pi/18 \ 0 \ 0]$ and $[0.05 \ 0 \ 0.01 \ -\pi/18 \ 0 \ 0]$. Although system state (presented in Figure 3 controlled by controller I), and system state (presented in Figure 4 controlled by controller II) all guarantee the system stability, it can be seen that the controller II makes the system perform a faster convergence rate for attitude angle α , β , μ than controller I, which implied better performance of disturbance suppression. The same situation can be seen in Figure 5 and Figure 6 as well.

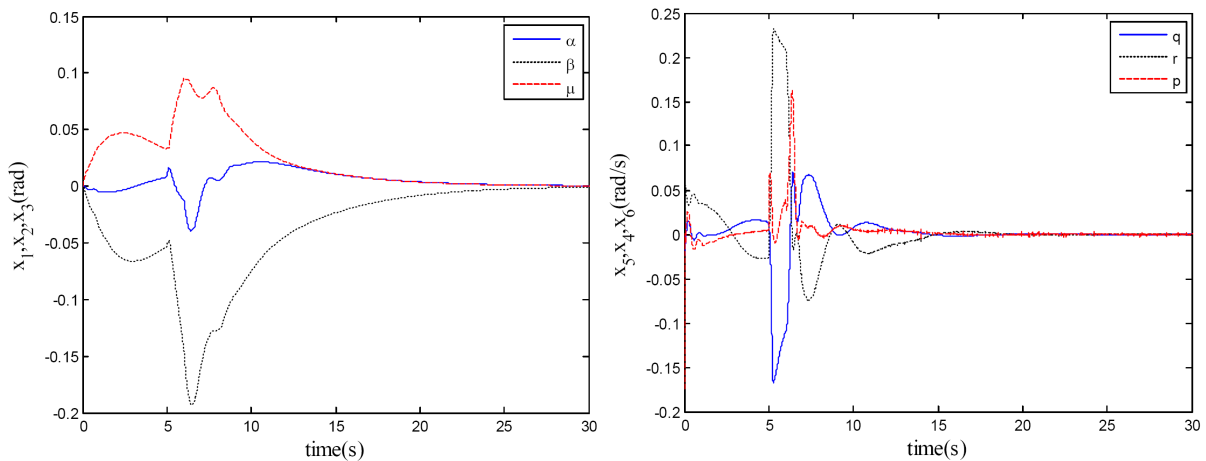


FIGURE 3. Response of the system state under the controller I at $[0 \ 0 \ 0 \ -\pi/18 \ 0 \ 0]$

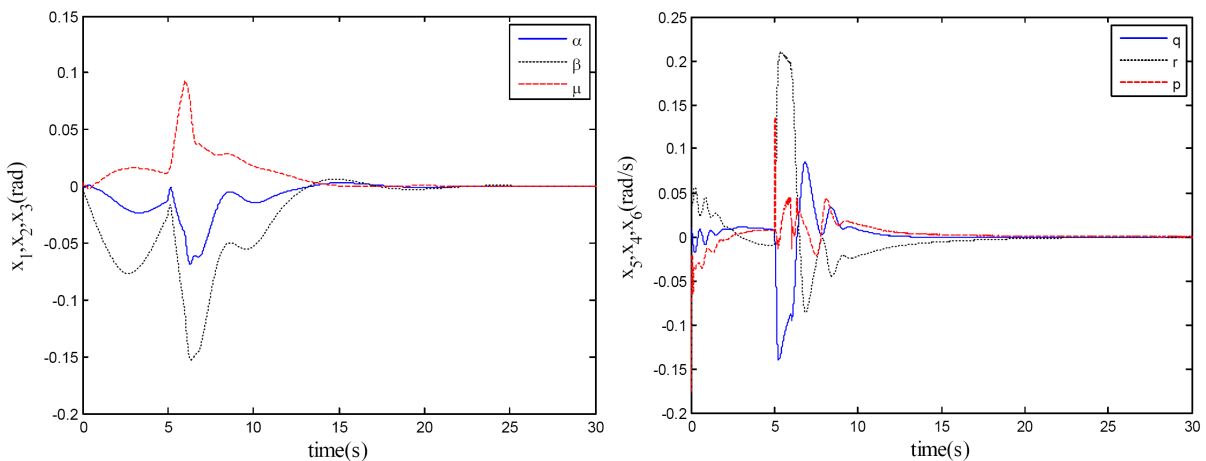


FIGURE 4. Response of the system state under the controller II at $[0 \ 0 \ 0 \ -\pi/18 \ 0 \ 0]$

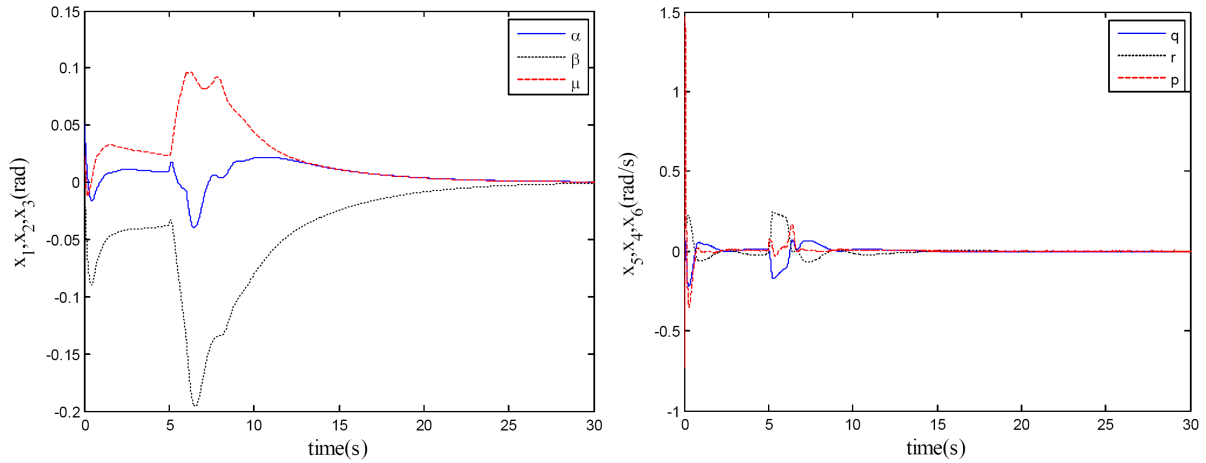


FIGURE 5. Response of the system state under the controller I at $[0.05 \ 0 \ 0.01 \ -\pi/18 \ 0 \ 0]$

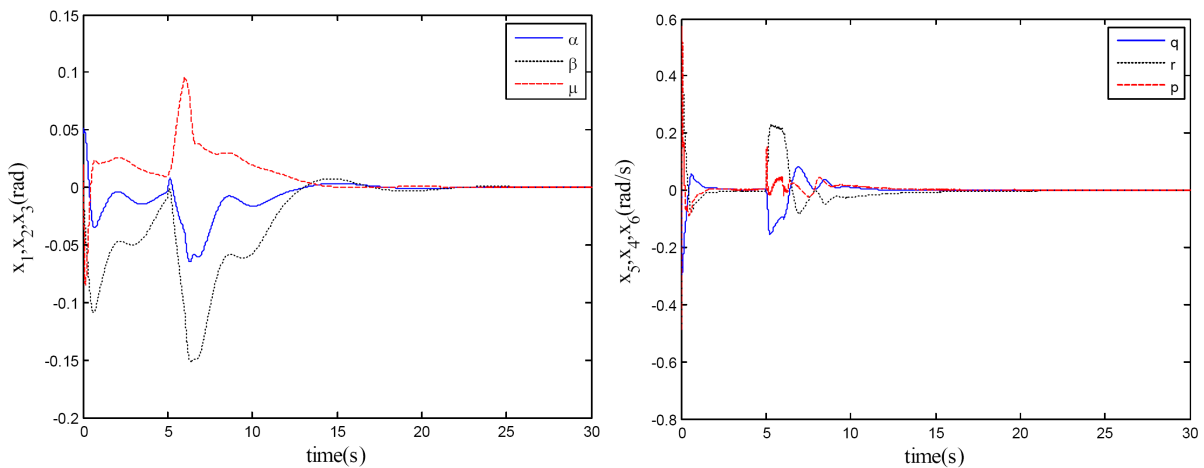


FIGURE 6. Response of the system state under the controller II at $[0.05 \ 0 \ 0.01 \ -\pi/18 \ 0 \ 0]$

On the other hand, as the attitude angular rates p , q , r for hypersonic vehicle are usually up-bounded, a smaller response of attitude angular rate will be more conducive to aircraft control and attitude stabilization. Compare the attitude angular rate of Figure 6 and Figure 7, as can be seen, when the response state number is increased, the response amplitude of the attitude angle rate of the controller I (value about 1.5 rad) shows much greater than that of the controller II (value about 0.6 rad), which means that the improved controller II ensures the system with more stable response performance, and a more reliable control effect at state point $[0.05 \ 0 \ 0.01 \ -\pi/18 \ 0 \ 0]$ is also achieved. This because that the introduction of the observation matrix in Equation (10) reduces the gain of the controller parameters and the design conservatism.

6. Conclusions. The H_∞ dynamic output feedback control of the HGV attitude system in reentry process has been addressed for the attitude dynamics model in three channels. The T-S uncertain fuzzy model of attitude dynamics is established first by T-S modeling technology. Then the T-S fuzzy output feedback controller with complete form of the HGV system with model uncertainties and external disturbances is designed based on

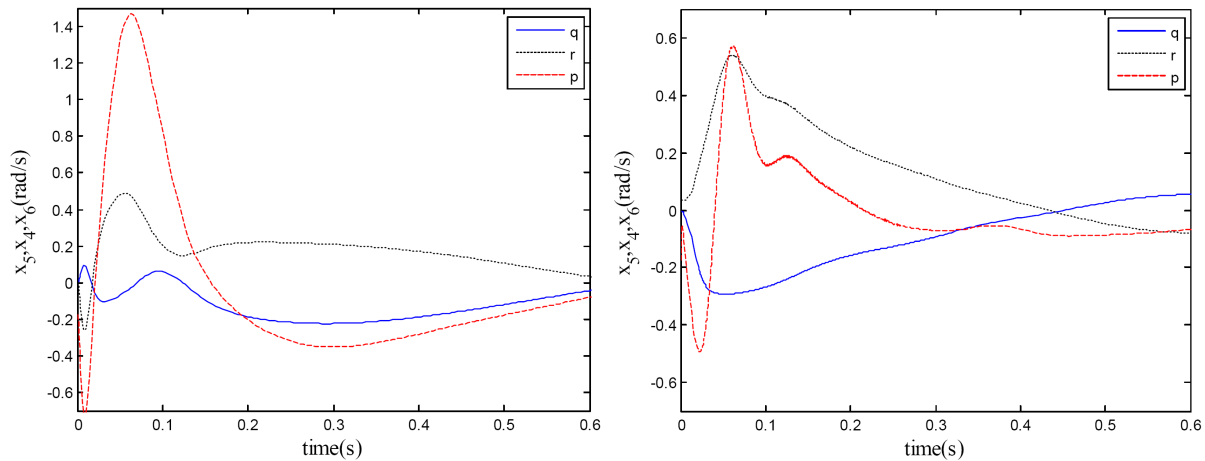


FIGURE 7. Local details of the attitude angular rate response at $[0.05 \ 0 \ 0.01 \ -\pi/18 \ 0 \ 0]$ (left: controller I, right: controller II)

partial state information when some states cannot be measured accurately in the flight process, and the strict LMI sufficient conditions are provided to calculate the controller parameters and ensure the system stability. Simulation results show that the designed controller has good dynamic performance when the system has uncertainties and external disturbances.

It is worth emphasizing that the dynamic output feedback controller proposed in this work is more practical compared with extant studies designed by full state feedback control. What is more, the introduction of T-S fuzzy strategy dramatically simplifies the complex system design, and the proposed strict LMI sufficient conditions make the control law easier to achieve and realize.

Acknowledgment. This work is supported by the National Natural Science Foundation of China [61273095].

REFERENCES

- [1] T. H. Phillips, A common aero vehicle (CAV) model, description, and employment guide, *Schafer Corporation for AFRL and AFSPC*, 2003.
- [2] S. Walker, J. Sherk, D. Shell et al., The DARPA/AF falcon program: The hypersonic technology vehicle #2 (HTV-2) flight demonstration phase, *The 15th AIAA International Space Planes and Hypersonic Systems and Technologies Conference*, pp.25-39, 2008.
- [3] V. V. Kislykh, A. A. Kondratov and V. L. Semenov, The program for the complex investigation of the hypersonic flight laboratory (HFL) "IGLA" in the PGU of TsNIIMash, *The 10th International Space Planes and Hyper Sonic Systems Conference*, Kyoto, Japan, pp.24-27, 2001.
- [4] P. Lu, S. Forbes and M. Baldwin, Gliding guidance of high L/D hypersonic vehicles, *AIAA Guidance, Navigation, and Control (GNC) Conference*, pp.46-48, 2013.
- [5] X. Chen, Z. Hou and J. Liu, Multi-objective optimization of reentry trajectory for hypersonic glide vehicle with multi-constraints, *Journal of National University of Defense Technology*, vol.31, no.6, pp.71-83, 2009.
- [6] S. Xue and P. Lu, Constrained predictor-corrector entry guidance, *Journal of Guidance Control & Dynamics*, vol.33, no.4, pp.1273-1281, 2010.
- [7] X. Liu, Y. Zhang, S. Wang and W. Huang, Backstepping attitude control for hypersonic gliding vehicle based on a robust dynamic inversion approach, *Proc. of the Institution of Mechanical Engineers Part I Journal of Systems and Control Engineering*, no.228, pp.543-552, 2014.
- [8] G. Cai, J. Song and X. Chen, Flight control system design for hypersonic reentry vehicle based on LFT-LPV method, *Proc. of the Institution of Mechanical Engineers Part G Journal of Aerospace Engineering*, no.228, pp.1130-1140, 2014.

- [9] X. Luo and J. Li, Fuzzy dynamic characteristic model based attitude control of hypersonic vehicle in gliding phase, *Science China Information Sciences*, vol.54, no.3, pp.448-459, 2011.
- [10] C. Qian, C. Sun, Y. Huang et al., Design of flight control system for a hypersonic gliding vehicle based on nonlinear disturbance observer, *IEEE International Conference on Control and Automation*, pp.1573-1577, 2013.
- [11] B. Xu, Robust adaptive neural control of flexible hypersonic flight vehicle with dead-zone input nonlinearity, *Nonlinear Dynamics*, vol.80, no.3, pp.1509-1520, 2015.
- [12] D. P. Wiese, A. M. Annaswamy, J. A. Muse et al., *Adaptive Control of a Generic Hypersonic Vehicle*, Massachusetts Institute of Technology, 2013.
- [13] H. B. Duan and P. Li, Progress in control approaches for hypersonic vehicle, *Science China Technological Sciences*, vol.55, no.10, pp.2965-2970, 2012.
- [14] B. Xu and Z. K. Shi, An overview on flight dynamics and control approaches for hypersonic vehicles, *Science China Information Sciences*, vol.58, no.7, pp.1-19, 2015.
- [15] H. Xu, M. Mirmirani and P. Ioannou, Adaptive sliding mode control design for a hypersonic flight vehicle, *Journal of Guidance Control and Dynamics*, vol.27, pp.829-838, 2004.
- [16] S.-G. Cao, N. W. Rees and G. Feng, Universal fuzzy controllers for a class of nonlinear systems, *Fuzzy Set. Syst.*, vol.122, pp.117-123, 2001.
- [17] C. Fantuzzi and R. Rovatti, On the approximation capabilities of the homogeneous Takagi-Sugeno model, *Proc. of the 5th IEEE Int. Conf. Fuzzy Syst.*, pp.1067-1072, 1996.
- [18] K. Zeng, N.-Y. Zhang and W.-L. Xu, A comparative study on sufficient conditions for Takagi-Sugeno fuzzy systems as universal approximators, *IEEE Trans. Fuzzy Syst.*, vol.8, pp.773-780, 2000.
- [19] J. Zhang, P. Shi and Y. Xia, Fuzzy delay compensation control for T-S fuzzy systems over network, *IEEE Trans. Cybernetics*, vol.43, no.1, pp.259-268, 2013.
- [20] H. Shen, J. H. Park and Z. G. Wu, Finite-time reliable $L_2 - L_\alpha/H_\alpha$ control for Takagi-Sugeno fuzzy systems with actuator faults, *IET Control Theory & Applications*, vol.8, no.9, pp.688-696, 2014.
- [21] D. Chen, W. Zhao, J. C. Sprott et al., Application of Takagi-Sugeno fuzzy model to a class of chaotic synchronization and anti-synchronization, *Nonlinear Dynamics*, vol.73, no.3, pp.1495-1505, 2013.
- [22] H. Li, H. Liu, H. Gao et al., Reliable fuzzy control for active suspension systems with actuator delay and fault, *IEEE Trans. Fuzzy Syst.*, vol.20, no.2, pp.342-357, 2012.
- [23] B. Jiang, Z. Gao, P. Shi et al., Adaptive fault-tolerant tracking control of near-space vehicle using Takagi-Sugeno fuzzy models, *IEEE Trans. Fuzzy Syst.*, vol.18, no.5, pp.1000-1007, 2010.
- [24] H. B. Li, Z. Q. Sun, H. B. Min et al., Fuzzy dynamic characteristic modeling and adaptive control of nonlinear systems and its application to hypersonic vehicles, *Science China Information Sciences*, vol.54, no.3, pp.460-468, 2011.
- [25] X. Hu, L. Wu, C. Hu et al., Fuzzy guaranteed cost tracking control for a flexible air-breathing hypersonic vehicle, *IET Control Theory & Applications*, vol.6, no.9, pp.1238-1249, 2012.
- [26] Y. N. Hu, Y. Yuan, H. B. Min et al., Multi-objective robust control based on fuzzy singularly perturbed models for hypersonic vehicles, *Science China Information Sciences*, vol.54, no.3, pp.563-576, 2011.
- [27] D. X. Gao and Z. Q. Sun, Fuzzy tracking control design for hypersonic vehicles via TS model, *Science China Information Sciences*, vol.54, no.3, pp.521-528, 2011.
- [28] J. C. Lo and M. L. Lin, Robust H_∞ nonlinear control via fuzzy static output feedback, *IEEE Trans. Circuits and Systems I: Fundamental Theory and Applications*, vol.50, no.11, pp.1494-1502, 2003.
- [29] C. Scherer, P. Gahinet and M. Chilali, Multiobjective output-feedback control via LMI optimization, *IEEE Trans. Autom. Control*, vol.42, no.7, pp.896-911, 1997.
- [30] G. H. Yang and J. Dong, Switching fuzzy dynamic output feedback H (infinity) control for nonlinear systems, *IEEE Trans. Systems Man & Cybernetics Part B Cybernetics A Publication of the IEEE Systems Man & Cybernetics Society*, vol.40, no.2, pp.505-516, 2010.
- [31] G. S. Deaecto, J. C. Geromel and J. Daafouz, Dynamic output feedback H_∞ control of switched linear systems, *Automatica*, vol.47, no.8, pp.1713-1720, 2011.
- [32] X. D. Li, B. Xian, C. Diao et al., Output feedback control of hypersonic vehicles based on neural network and high gain observer, *Science China Information Sciences*, vol.54, no.3, pp.429-447, 2011.
- [33] Q. Zong, Y. Ji, F. Zeng et al., Output feedback back-stepping control for a generic hypersonic vehicle via small-gain theorem, *Aerospace Science and Technology*, vol.23, no.1, pp.409-417, 2012.
- [34] D. Sigthorsson, P. Jankovský, A. Serrani et al., Robust linear output feedback control of an airbreathing hypersonic vehicle, *Journal of Guidance Control & Dynamics*, vol.31, no.31, pp.1052-1066, 2012.

- [35] D. P. Wiese, A. M. Annaswamy, J. A. Muse et al., Adaptive output feedback based on closed-loop reference models for hypersonic vehicles, *Journal of Guidance Control & Dynamics*, vol.38, no.12, pp.1-12, 2015.
- [36] X. Hu, L. Wu, C. Hu et al., Dynamic output feedback control of a flexible air-breathing hypersonic vehicle via T-S fuzzy approach, *International Journal of Systems Science*, vol.45, no.8, pp.1740-1756, 2014.
- [37] Y. Chang, X. Wang, H. E. Chun et al., Study on adaptive variable structure control law for hypersonic gliding vehicle, *Aerospace Control*, 2015.
- [38] K. Gao, Q. Li, Z. Ren et al., Observer-based attitude control for hypersonic gliding vehicle, *Guidance, Navigation and Control Conference*, pp.1159-1162, 2014.
- [39] C. Bai, C. Lian, Z. Ren et al., Adaptive tracking control of hypersonic reentry vehicle with uncertain parameters, *The 3rd International Conference on Instrumentation, Measurement, Computer, Communication and Control*, pp.1594-1597, 2013.
- [40] I. E. Mooij, *The Motion of a Vehicle in a Planetary Atmosphere*, Delft University of Technology, 1997.
- [41] M. C. M. Teixeira and S. H. Zak, Stabilizing controller design for uncertain nonlinear systems using fuzzy models, *IEEE Trans. Fuzzy Syst.*, vol.7, no.2, pp.133-142, 1999.
- [42] S. Chae and S. K. Nguang, SOS based robust fuzzy dynamic output feedback control of nonlinear networked control systems, *IEEE Trans. Cybernetics*, vol.44, no.7, pp.1204-1213, 2014.
- [43] I. R. Petersen, A stabilization algorithm for a class of uncertain linear systems, *Systems & Control Letters*, vol.8, no.4, pp.351-357, 1987.
- [44] H. D. Tuan, P. Apkarian, T. Narikiyo et al., Parameterized linear matrix inequality techniques in fuzzy control system design, *IEEE Trans. Fuzzy Syst.*, vol.9, no.2, pp.324-332, 2001.
- [45] Y. H. Wang, Q. X. Wu, C. S. Jiang et al., Fuzzy robust tracking control for aerospace vehicle's reentry attitude based on fuzzy feedforward, *Journal of Astronautics*, vol.29, no.1, pp.156-161, 2008.

Appendix.

$$\begin{aligned}
 \mathbf{A}_1 &= \begin{bmatrix} 0 & 0.17453 & 0 & 0 & 1 & 0 \\ -0.17453 & 0 & 0 & 0 & 0 & -1 \\ 0.17453 & 0 & 0 & -1 & 0 & 0 \\ 0 & 0 & 0 & 0 & 1253.5 & 0 \\ 0 & 0 & 0 & 0.011223 & 0 & -0.17222 \\ 0 & 0 & 0 & 0 & 332.21 & 0 \end{bmatrix} \\
 \mathbf{A}_2 &= \begin{bmatrix} 0 & 0.17453 & 0 & 0 & 1 & 0 \\ -0.17453 & 0 & 0 & 0 & 0 & -1 \\ 0 & 0 & 0 & -1 & 0 & 0 \\ 0 & 0 & 0 & 0 & -451.69 & 0 \\ 0 & 0 & 0 & 0.04586 & 0 & -0.16099 \\ 0 & 0 & 0 & 0 & -119.48 & 0 \end{bmatrix} \\
 \mathbf{A}_3 &= \begin{bmatrix} 0 & 0.17453 & 0 & 0 & 1 & 0 \\ -0.17453 & 0 & 0 & 0 & 0 & -1 \\ -0.17453 & 0 & 0 & -1 & 0 & 0 \\ 0 & 0 & 0 & 0 & -2156.9 & 0 \\ 0 & 0 & 0 & 0.17222 & 0 & 0.011223 \\ 0 & 0 & 0 & 0 & -571.17 & 0 \end{bmatrix} \\
 \mathbf{A}_4 &= \begin{bmatrix} 0 & 0 & 0 & 0 & 1 & 0 \\ 0 & 0 & 0 & 0 & 0 & -1 \\ 0.17453 & 0 & 0 & -1 & 0 & 0 \\ 0 & 0 & 0 & 0 & 1705.2 & 0 \\ 0 & 0 & 0 & -0.16099 & 0 & -0.04586 \\ 0 & 0 & 0 & 0 & 451.69 & 0 \end{bmatrix}
 \end{aligned}$$

$$\begin{aligned}
\mathbf{A}_5 &= \begin{bmatrix} 0 & 0 & 0 & 0 & 1 & 0 \\ 0 & 0 & 0 & 0 & 0 & -1 \\ 0 & 0 & 0 & -1 & 0 & 0 \\ 0 & 0 & 0 & 0 & 0 & 0 \\ 0 & 0 & 0 & 0 & 0 & 0 \\ 0 & 0 & 0 & 0 & 0 & 0 \end{bmatrix} \\
\mathbf{A}_6 &= \begin{bmatrix} 0 & 0 & 0 & 0 & 1 & 0 \\ 0 & 0 & 0 & 0 & 0 & -1 \\ -0.17453 & 0 & 0 & -1 & 0 & 0 \\ 0 & 0 & 0 & -1705.2 & 0 & 0 \\ 0 & 0 & 0 & 0.16099 & 0 & 0.04586 \\ 0 & 0 & 0 & 0 & -451.69 & 0 \end{bmatrix} \\
\mathbf{A}_7 &= \begin{bmatrix} 0 & -0.17453 & 0 & 0 & 1 & 0 \\ 0.17453 & 0 & 0 & 0 & 0 & -1 \\ 0.17453 & 0 & 0 & -1 & 0 & 0 \\ 0 & 0 & 0 & 2156.9 & 0 & 0 \\ 0 & 0 & 0 & -0.17222 & 0 & -0.011223 \\ 0 & 0 & 0 & 0 & 571.17 & 0 \end{bmatrix} \\
\mathbf{A}_8 &= \begin{bmatrix} 0 & -0.17453 & 0 & 0 & 1 & 0 \\ 0.17453 & 0 & 0 & 0 & 0 & -1 \\ 0 & 0 & 0 & -1 & 0 & 0 \\ 0 & 0 & 0 & 451.69 & 0 & 0 \\ 0 & 0 & 0 & -0.04586 & 0 & -0.16099 \\ 0 & 0 & 0 & 0 & 119.48 & 0 \end{bmatrix} \\
\mathbf{A}_9 &= \begin{bmatrix} 0 & -0.17453 & 0 & 0 & 1 & 0 \\ 0.17453 & 0 & 0 & 0 & 0 & -1 \\ -0.17453 & 0 & 0 & -1 & 0 & 0 \\ 0 & 0 & 0 & 0 & -1253.5 & 0 \\ 0 & 0 & 0 & -0.011223 & 0 & 0.17222 \\ 0 & 0 & 0 & 0 & -332.21 & 0 \end{bmatrix} \\
\mathbf{B}_i &= \begin{bmatrix} 0 & 0 & 0 \\ 0 & 0 & 0 \\ 0 & 0 & 0 \\ 31.983 & 0 & 8.4714 \\ 0 & 0.0002 & 0 \\ 8.4714 & 0 & 2.244 \end{bmatrix}, \quad i = 1, 2, \dots, 9
\end{aligned}$$